

Uncertainty of the astrophysical $^{17,18}\text{O}(\alpha, n)^{20,21}\text{Ne}$ reaction rates and the applicability of the statistical model for nuclei with $A \lesssim 20$

Peter Mohr*

*Diakonie-Klinikum, D-74523 Schwäbisch Hall, Germany
and Institute for Nuclear Research (Atomki), H-4001 Debrecen, Hungary*

(Received 30 June 2017; published 13 October 2017)

Background: The (α, n) , and (α, γ) reactions on $^{17,18}\text{O}$ have significant impact on the neutron balance in the astrophysical s process. In this scenario stellar reaction rates are required for relatively low temperatures below $T_9 \lesssim 1$.

Purpose: The uncertainties of the $^{17,18}\text{O}(\alpha, n)^{20,21}\text{Ne}$ reactions are investigated. Statistical model calculations are performed to study the applicability of this model for relatively light nuclei in extension to a recent review for the $20 \leq A \leq 50$ mass range.

Method: The available experimental data for the $^{17,18}\text{O}(\alpha, n)^{20,21}\text{Ne}$ reactions are compared with statistical model calculations. Additionally, the reverse $^{20}\text{Ne}(n, \alpha)^{17}\text{O}$ reaction is investigated, and similar studies for the ^{17}F mirror nucleus are provided.

Results: It is found that, on average, the available experimental data for ^{17}O and ^{18}O are well described within the statistical model, resulting in reliable reaction rates above $T_9 \gtrsim 1.5$ from these calculations. However, significant experimental uncertainties are identified for the $^{17}\text{O}(\alpha, n_0)^{20}\text{Ne}$ (ground state) channel.

Conclusions: The statistical model is able to predict astrophysical reaction rates for temperatures above 1 GK with uncertainties of less than a factor of two for the nuclei under study. An experimental discrepancy for the $^{17}\text{O}(\alpha, n)^{20}\text{Ne}$ reaction needs to be resolved.

DOI: [10.1103/PhysRevC.96.045808](https://doi.org/10.1103/PhysRevC.96.045808)

I. INTRODUCTION

α -induced reactions play an important role in various astrophysical scenarios. In the astrophysical s process, the $^{13}\text{C}(\alpha, n)^{16}\text{O}$ and $^{22}\text{Ne}(\alpha, n)^{25}\text{Mg}$ reactions are the neutron production reactions [1], and the $^{17}\text{O}(\alpha, n)^{20}\text{Ne}$, $^{17}\text{O}(\alpha, \gamma)^{21}\text{Ne}$, and $^{18}\text{O}(\alpha, n)^{21}\text{Ne}$ reactions affect the neutron balance via the potential neutron poison ^{16}O . Depending on the rates of these reactions, a neutron may be first absorbed by the highly abundant ^{16}O nucleus in the $^{16}\text{O}(n, \gamma)^{17}\text{O}$ reaction, but later the neutron can be recycled in the $^{17}\text{O}(\alpha, n)^{20}\text{Ne}$ reaction [2,3].

In most cases the statistical model (StM) is applied for the calculation of α -induced reaction rates. The StM is well founded for heavy target nuclei, e.g., for (α, n) reactions under certain r -process conditions [4–6], and for inverse (γ, α) reactions in the γ process [7,8]. Contrary to the situations in the r process and γ process, it is not clear whether the level density is sufficiently high for a reliable calculation of α -induced reactions for the light target nuclei in the s process with masses $A \lesssim 20$. Interestingly, it was found that the reaction cross sections in the $20 \leq A \leq 50$ mass range follow a generic behavior and can be quite well described within the StM [9] by using the simple four-parameter potential by McFadden and Satchler [10]. This holds in particular for slightly higher energies and/or nuclei at the upper end of the $20 \leq A \leq 50$ mass range. For low energies and lighter target nuclei, the cross sections are dominated by individual resonances, and thus the StM is only able to reproduce the average trend of the experimental cross sections. Contrary to this excellent performance for light target nuclei, the simple

McFadden–Satchler potential tends to overpredict α -induced cross sections for heavy target nuclei in the $A \approx 100$ mass range and above. Much effort has been spent in the recent years to provide improved global α -nucleus potentials for heavy nuclei, and significant improvements have been achieved (see, e.g., Refs. [11–15]).

Primarily, this study was motivated as an extension of the previous review in the $20 \leq A \leq 50$ mass range [9] with the aim to provide a prediction for the upcoming $^{17}\text{F}(\alpha, p)^{20}\text{Ne}$ data which have been measured recently by using the MUSIC chamber at Argonne National Laboratory (ANL) [16,17]. A further experiment for $^{17}\text{F}(\alpha, p)^{20}\text{Ne}$ has been done at Florida State University using the ANASEN active detector [18]. In the course of this study of $^{17}\text{F} + \alpha$, the mirror $^{17}\text{O}(\alpha, n)^{20}\text{Ne}$ reaction was also analyzed, and unexpected inconsistencies between different experimental data sets were identified. These are based on the $^{17}\text{O}(\alpha, n)^{20}\text{Ne}$ data in Refs. [19–24] and the reverse $^{20}\text{Ne}(n, \alpha)^{17}\text{O}$ reaction [25–28]. As a consequence, the present work now focuses on the resulting uncertainties of the $^{17}\text{O}(\alpha, n)^{20}\text{Ne}$ reaction rate. In most cases [19,20,22,23,29] the same experimental techniques were also applied to the $^{18}\text{O}(\alpha, n)^{21}\text{Ne}$ reaction. This allows a careful comparison of the experimental results for two nuclei, and in addition a step-by-step extension of the systematics in the $20 \leq A \leq 50$ mass range [9] towards lighter nuclei is possible. Detailed calculations of the $^{17}\text{F}(\alpha, p)^{20}\text{Ne}$ and its reverse $^{20}\text{Ne}(p, \alpha)^{17}\text{F}$ reaction [30] will be provided in a separate paper [16]. Most experimental data in this work have been taken from the EXFOR database [31]; other sources are given explicitly.

The paper is organized as follows: Sec. II gives a review of the existing experimental data for the $^{18}\text{O}(\alpha, n)^{21}\text{Ne}$ reaction,

*WidmaierMohr@t-online.de; mohr@atomki.mta.hu

and the experimental data are compared with StM calculations. Section III provides a similar review for the $^{17}\text{O}(\alpha, n)^{20}\text{Ne}$ reaction which is extended by data for the reverse $^{20}\text{Ne}(n, \alpha)^{17}\text{O}$ reaction. The $^{17}\text{F}(\alpha, p)^{20}\text{Ne}$ and $^{20}\text{Ne}(p, \alpha)^{17}\text{F}$ reactions are briefly mentioned in Sec. IV. Astrophysical reaction rates are calculated, and their uncertainties are discussed in Sec. V. Finally, because the α -nucleus potential is the key ingredient for the calculation of (α, n) cross sections, the results from different α -nucleus potentials are presented in Sec. VI. Conclusions are drawn in Sec. VII.

The StM calculations in the present work were made using the code TALYS [32] (version 1.8) in combination with the α -nucleus potential by McFadden–Satchler. This choice is based on the excellent performance of the McFadden–Satchler potential in the $20 \leq A \leq 50$ mass range [9] and on the finding that most of the recent global potentials [11–13] provide relatively similar cross sections for lighter nuclei [33]. Other ingredients for the StM calculations, such as the nucleon optical model potential, the γ -ray strength function, and the level density, have very minor influence on the calculated (α, n) or (α, p) cross sections within the StM, in particular as long as either the (α, n) or the (α, p) channel has a dominating contribution to the total α -induced reaction cross section; this is often the case in the $20 \leq A \leq 50$ mass range [9]. Although the role of the chosen level-density parametrization in the StM calculations is minor, in reality, at the lowest energies under study, the cross sections are governed by the properties of few levels which appear as low-energy resonances in the (α, n) cross section.

II. $^{18}\text{O}(\alpha, n)^{21}\text{Ne}$

The present study starts from the first NACRE compilation [34] in 1999; the updated NACRE-2 compilation [35] ends at $A = 16$ and does not include the reactions under analysis. NACRE lists four experiments where total $^{18}\text{O}(\alpha, n)^{21}\text{Ne}$ cross sections were measured by neutron counting. This technique does not provide much information on the neutron energy, which complicates a precise calibration of the energy-dependent efficiency of the neutron longcounters. In addition, resonances in background reactions may be misinterpreted. Nevertheless, the four data sets by Bair and Willard [36] (hereafter Bair62; the other data sets are referenced by the first author in the following), Hansen *et al.* [19], Bair and Haas [20], and Denker [22] are in reasonable agreement (see Fig. 1). The data cover energies from close above the reaction threshold up to about 10 MeV. Note that the $^{18}\text{O}(\alpha, n)^{21}\text{Ne}$ reaction has a slightly negative Q value of $Q = -698$ keV, leading to a threshold at $E_\alpha = 842$ keV in the laboratory system.

The TALYS calculations show good agreement with the Hansen data at higher energies above 5 MeV, and the calculations reproduce the average trend of the Bair62 data down to about 2 MeV. At even lower energies, there is still reasonable agreement between the calculation and the average trend of the Bair data and the Denker data.

In addition to the longcounter data, time-of-flight (TOF) data have been used by Hansen *et al.* [19] at higher energies around 10 MeV to discriminate between the final states in the residual ^{21}Ne nucleus. The resolution was not sufficient to

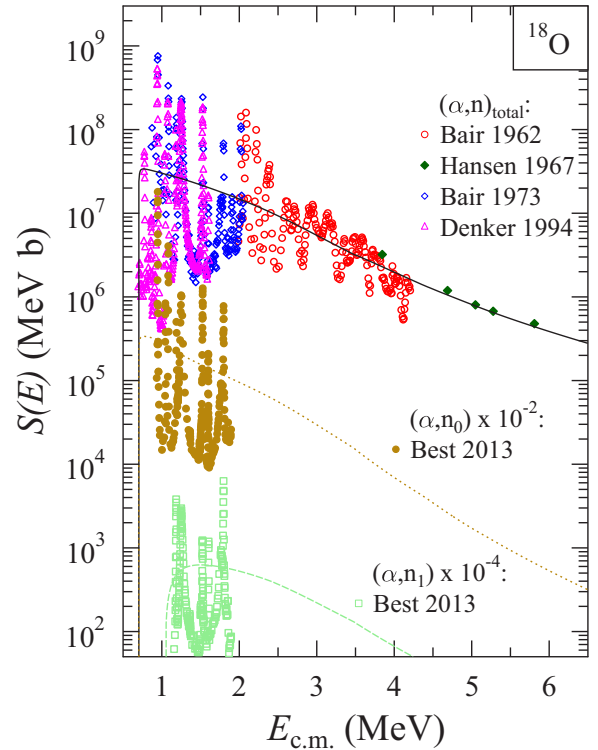


FIG. 1. Total $^{18}\text{O}(\alpha, n)^{21}\text{Ne}$ S factor from neutron counting experiments [19,20,22,36] and partial (α, n_0) and (α, n_1) cross section measurements [29] in comparison to TALYS calculations. The (α, n_0) and (α, n_1) data are scaled by factors of 10^{-2} and 10^{-4} for better visibility. For further discussion see text.

resolve all individual levels of ^{21}Ne ; only angular distributions for three groups ($n_0 + n_1$; $n_2 + n_3$; $n_5 + n_6 + n_7$) are shown in Ref. [19]. The angle-integrated cross sections of these groups are in reasonable agreement with the TALYS calculations with deviations below a factor of two in all cases. In particular, the $(n_0 + n_1)$ group with cross sections of about 80 to 45 mb from 9.8 to 12.3 MeV are nicely reproduced within about 20%, giving some confidence in the calculated branching ratios to the lowest states in ^{21}Ne .

The latest study by Best *et al.* [29] at low energies improves the previous longcounter measurements by an additional determination of the $^{18}\text{O}(\alpha, n_1)^{21}\text{Ne}$ cross section by γ -ray spectroscopy. The information from the γ -ray data on the (α, n_1) cross section is used to calculate the contribution of the (α, n_1) channel to the total neutron yield which is measured as in the other studies by neutron counting. After subtraction of the (α, n_1) yield, the remaining yield is assigned to the (α, n_0) channel (other channels are closed for the low energies under study in Ref. [29]), and this remaining yield is then converted to the (α, n_0) cross section with smaller uncertainties because the neutron energy in the (α, n_0) channel is now known from kinematics; thus, the neutron detection efficiency can be determined with improved accuracy.

The total $^{18}\text{O}(\alpha, n)^{21}\text{Ne}$ cross section of the Best data is in good agreement with the other data sets, and also the branching ratio between the (α, n_0) and (α, n_1) cross sections is on average well reproduced by the TALYS calculations

(see Fig. 1); obviously, the branching ratio of the individual resonances cannot be reproduced by the StM calculations. This leads to three conclusions for the $^{18}\text{O}(\alpha, n)^{21}\text{Ne}$ reaction: First, this cross section is well determined experimentally from several data sets which agree with each other [19,20,22,29,36]. Second, the statistical model is able to predict the average cross section for both open channels at low energies. Third, the excellent performance of the simple α -nucleus potential of McFadden and Satchler [10] in the $20 \leq A \leq 50$ mass range [9] can at least be extended down to ^{18}O .

III. $^{17}\text{O}(\alpha, n)^{20}\text{Ne}$

From the above conclusions on the $^{18}\text{O}(\alpha, n)^{21}\text{Ne}$ reaction, similar findings are expected for the $^{17}\text{O}(\alpha, n)^{20}\text{Ne}$ reaction because the same experimental techniques have been applied by the same groups. However, this is not the case. The available experimental data are in part contradictory for the $^{17}\text{O}(\alpha, n)^{20}\text{Ne}$ reaction.

Similar to $^{18}\text{O}(\alpha, n)^{21}\text{Ne}$, the starting point of the present analysis is the NACRE compilation from 1999. Three data sets are listed, starting with the early work of Hansen *et al.* [19], the data by Bair and Haas [20], and the unpublished data by Denker [22]. All experiments use simple neutron counting techniques. Similar to the ^{18}O case, the three data sets are in reasonable agreement (see Fig. 2). Very recently, Avila *et al.* [24] have measured the $^{17}\text{O}(\alpha, n)^{20}\text{Ne}$ reaction in inverse kinematics by the detection of the residual ^{20}Ne nucleus for energies corresponding to $E_\alpha \approx 3\text{--}6$ MeV. Also, these data with their completely different systematic uncertainties agree well in the overlap regions with the Bair data and the Hansen data. The TALYS calculation is able to reproduce the experimental data at higher energies. At lower energies the cross section is dominated by individual resonances, but still the statistical model calculations reproduce the average trend of the data.

Again similar to the ^{18}O case, Hansen *et al.* [19] have applied the TOF technique to discriminate between the final states in ^{20}Ne . Angular distributions for the n_1 , the n_2 , and the sum of the ($n_4 + n_5$) channels are shown for energies between 9.8 and 12.3 MeV, and it is pointed out that the n_0 channel and the n_3 channel are only weakly populated, thus preventing an analysis. The experimental data points for the n_1 and n_2 channels (from 9.8 to 12.3 MeV: about 80 to 30 mb for the n_1 channel and 90 to 70 mb for the n_2 channel) are reproduced by the TALYS calculations with deviations below about 20%, and the calculated n_0 cross section is about a factor of five lower than the n_1 channel. This confirms the TALYS calculations for the branchings to individual final states in ^{20}Ne .

Again similar to the ^{18}O case, Best *et al.* [23] have extended the neutron counting experiments by an additional measurement of the $^{17}\text{O}(\alpha, n_1)^{20}\text{Ne}$ reaction by γ spectroscopy of the 1634 keV γ ray from the decay of the first-excited state in ^{20}Ne to the ground state. The (α, n_1) data at low energies are on average well reproduced by the TALYS calculations. Then, Best *et al.* calculate the yield of the (α, n_1) reaction in their neutron detector, and from the difference of the measured yield and the calculated (α, n_1) yield the (α, n_0) cross section is extracted. Other channels are closed at the energies under study in Ref. [23]. Contrary to the TOF results by Hansen *et al.* [19]

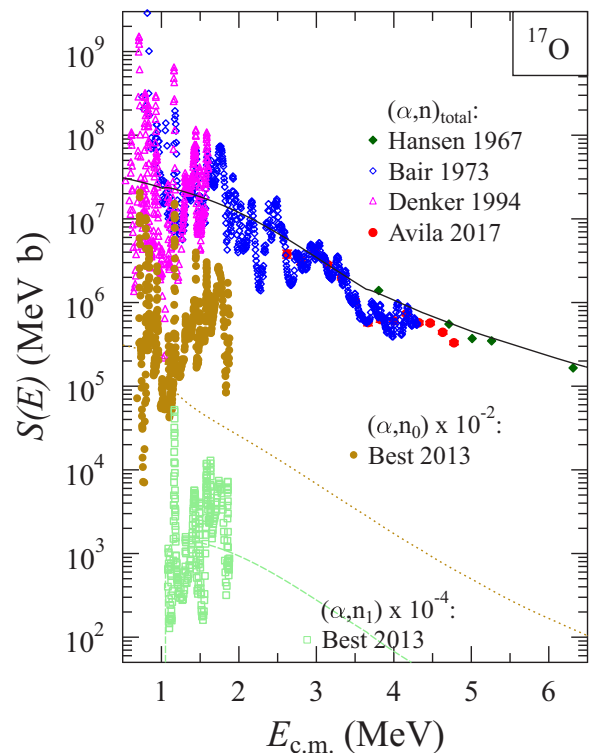


FIG. 2. Total $^{17}\text{O}(\alpha, n)^{20}\text{Ne}$ S factor from neutron counting experiments [19,20,22] and partial (α, n_0) and (α, n_1) cross section measurements [29] in comparison with TALYS calculations [total (α, n) shown by full black line; (α, n_0) shown by golden dotted line; (α, n_1) shown by light green dashed line]. Further total (α, n) data are measured by detection of the ^{20}Ne recoil nucleus in inverse kinematics [24]. The (α, n_0) and (α, n_1) data are scaled by factors of 10^{-2} and 10^{-4} for better visibility. For further discussion see text.

around 10 MeV, it is found for the low-energy region that the n_0 channel is dominating over the n_1 channel. As can be seen from Fig. 2, the TALYS calculation is significantly lower than the experimental result for the (α, n_0) channel. Interestingly, this discrepancy between the Best data for the n_0 channel and the TALYS calculation appears mainly in the energy region above the opening of the n_1 channel (see Fig. 3).

It is somewhat difficult to visualize the essential discrepancies between the various experimental data sets; an attempt is made in Fig. 3. Above the n_1 threshold at $E_{c.m.} = 1047$ keV and clearly visible above about 1.3 MeV, the Best (α, n_0) data exceed the total (α, n) data of Bair and of Denker by about a factor of three. The TALYS calculation predicts on average a weak n_0 channel and a dominating n_1 channel whereas the Best data show the opposite trend over the whole energy range. Note that the TALYS predictions are verified around 10 MeV according to the Hansen TOF data.

There is an additional experiment by McDonald *et al.* [21] on isospin-forbidden particle decays in ^{21}Ne . An attempt was made in Ref. [21] to find weak $T = 3/2$ resonances in the $^{17}\text{O}(\alpha, n_0)^{20}\text{Ne}$ channel by neutron detection in an energy-sensitive NE213 scintillator and in the $^{17}\text{O}(\alpha, n_1)^{20}\text{Ne}$ channel by γ spectroscopy. As a byproduct, neighboring strong

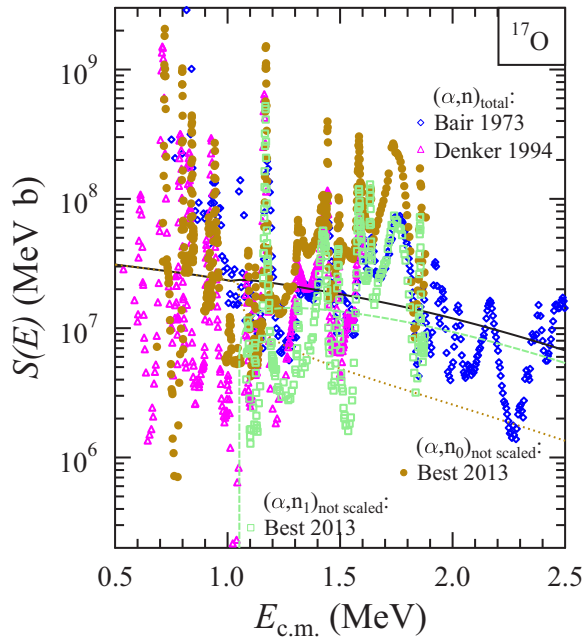


FIG. 3. Same as Fig. 2 for low energies. Above the opening of the n_1 channel at $E_\alpha = 1293$ keV ($E_{c.m.} = 1047$ keV), the Best data for the n_0 channel exceed the Bair and the Denker data and are also significantly above the TALYS prediction (golden dotted line). Below the n_1 threshold, the experimental data sets roughly agree. Note that, contrary to Fig. 2, the (α, n_0) and (α, n_1) data are not scaled. For further discussion see text.

$T = 1/2$ resonances were also seen in Ref. [21]. In particular, two resonances are discussed explicitly in Ref. [21].

At $E_{c.m.} = 1491$ keV a resonance was found in the (α, n_1) channel, but no enhanced yield was seen in the (α, n_0) channel. $\Gamma_{n_0}/\Gamma < 0.3$ was deduced from the data, in conflict with the Best data which give $\Gamma_{n_0} = 5.13$ keV and $\Gamma_{n_1} = 3.05$ keV, leading to $\Gamma_{n_0}/\Gamma_{n_1} = 1.68$. For completeness it should be noted that the Denker data for the total (α, n) cross section agree almost perfectly with the Best data for the (α, n_1) channel around the 1491 keV resonance.

For the tail of the broad resonance at $E_{c.m.} = 1753$ keV ($E_\alpha = 2165$ keV) differential cross sections of slightly below 2 mb/sr are given at $E_\alpha \approx 2200$ keV for the (α, n_0) and the (α, n_1) channels in Ref. [21]. Assuming isotropy, this corresponds to angle-integrated cross sections of the order of 20–25 mb. Interestingly, the (α, n_1) cross section is in rough agreement with the Best data, but the (α, n_0) cross section is again significantly lower (by about a factor of two) than the Best result.

The reverse $^{20}\text{Ne}(n, \alpha)^{17}\text{O}$ reaction can be used to provide a further constraint on the $^{17}\text{O}(\alpha, n_0)^{20}\text{Ne}$ data. This possibility was unfortunately disregarded in the previous works [23,34]. Three data sets are available for neutrons in the low-MeV energy region. The early data by Johnson *et al.* [25] are composed of the α_0 and α_1 channels and cover the low-energy region. Bell *et al.* [26] are able to resolve the α_0 and α_1 channels for low neutron energies between 3 and 4.5 MeV; at higher energies also only the sum of the first two channels is reported.

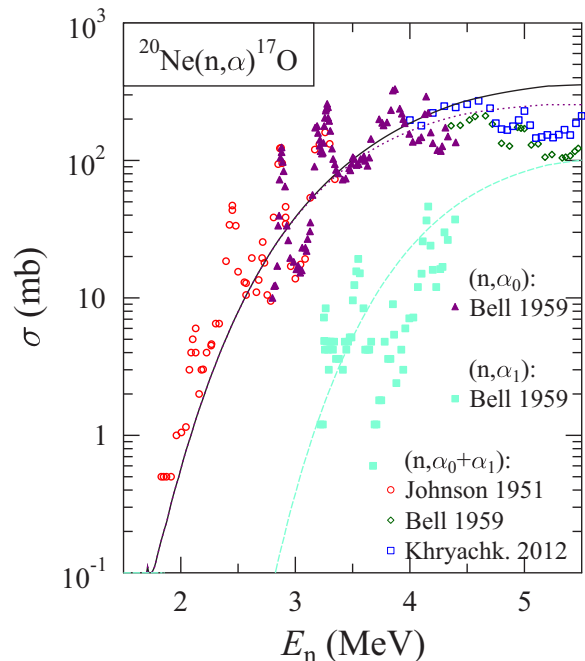


FIG. 4. Experimental cross section of the $^{20}\text{Ne}(n, \alpha)^{17}\text{O}$ reaction [25–28] in comparison to a statistical model calculation. Because of the dominating α_0 channel, the (n, α) data provide an additional constraint for the $^{17}\text{O}(\alpha, n_0)^{20}\text{Ne}$ cross section.

At energies above 4 MeV, recently Khryachkhov *et al.* [27,28] have also measured the sum of the α_0 and α_1 channels. The (n, α) data are in good agreement below 5 MeV (see Fig. 4) although at higher energies discrepancies up to about a factor of two are found. The Bell data clearly indicate that the (n, α_0) channel is dominating with a minor contribution of the (n, α_1) channel of the order of 10%. Higher-lying final states in ^{17}O do not play a role at energies below 5 MeV.

The TALYS calculations are able to reproduce the average trend of the experimental data. The agreement is very good for the (n, α_0) channel between 3 and 4 MeV, corresponding to slightly lower energies E_α in the (α, n) reaction because of the small negative Q value of the (n, α) reaction of $Q = -587$ keV.

The $^{20}\text{Ne}(n, \alpha_0)^{17}\text{O}$ data can be converted to $^{17}\text{O}(\alpha, n_0)^{20}\text{Ne}$ cross sections by application of the reciprocity theorem. The comparison between the Best data for the (α, n_0) channel and the converted (n, α) data of Johnson and Bell is shown in Fig. 5. A significant discrepancy can be seen between the Best data and the data from the reverse (n, α) reaction. For completeness also the TALYS calculation for the (α, n_0) channel is included in Fig. 5 which clearly favors the lower data from the (n, α) reaction.

Summarizing the above results, there is a clear experimental contradiction between the Best data for the (α, n_0) channel on the one hand and the (α, n) data of McDonalds and the (n, α) data of Johnson and of Bell on the other hand. The TALYS calculation clearly favors the lower (α, n_0) data of McDonalds, Johnson, and Bell. The (α, n_0) data of Best are also above the total (α, n) data of Denker and Bair [at least above the (α, n_1) threshold]. Thus, the simplest approach for consistency

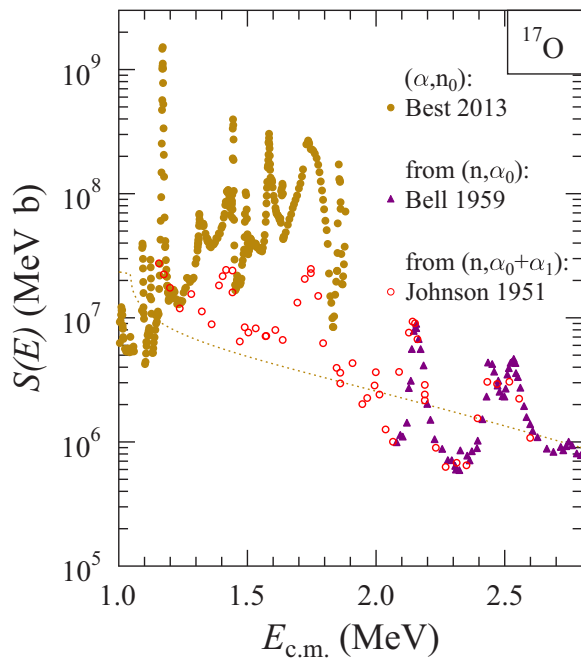


FIG. 5. Same as Fig. 2 for the overlap region between the Best data for the (α, n_0) channel and the converted (n, α) data of Johnson *et al.* [25] and Bell *et al.* [26]. The (α, n_0) data are in significant disagreement with the (n, α) data. The TALYS calculation reproduces the average trend of the (n, α) data. For further discussion see text.

is a reduction of the (α, n_0) data of Best above the (α, n_1) threshold by a significant amount. Typically, this reduction should be at least a factor of two to three (but an energy-independent reduction factor may be inappropriate). Any other solution would require the modification of several data sets which are roughly consistent with each other. Fortunately, new experiments for the $^{17}\text{O}(\alpha, n)^{20}\text{Ne}$ reaction are in preparation [37] using improved energy-sensitive neutron detectors [38].

IV. $^{17}\text{F}(\alpha, p)^{20}\text{Ne}$

A detailed discussion of the $^{17}\text{F}(\alpha, p)^{20}\text{Ne}$ reaction will be given in a forthcoming paper with the upcoming experimental results from ANL [16]. As a first step, the reverse $^{20}\text{Ne}(p, \alpha)^{17}\text{F}$ reaction was studied. Figure 6 shows the experimental results of Gruhle *et al.* [30] for the total (p, α) cross section. The TALYS calculation is again able to reproduce the data quite well.

According to TALYS, the (p, α_0) channel is dominating over the whole energy range of the Gruhle data with a small contribution ($\lesssim 20\%$) from the (p, α_1) channel and negligible contributions from higher-lying channels like (p, α_2) . Such a branching ratio is expected from the negative Q value of the (p, α) reaction and the resulting strong Coulomb suppression of the higher-lying final states in ^{17}F .

Because of the dominance of the (p, α_0) channel, the experimental (p, α) data can be approximately converted to the $^{17}\text{F}(\alpha, p_0)^{20}\text{Ne}$ cross section. However, a comparison with the upcoming $^{17}\text{F}(\alpha, p)^{20}\text{Ne}$ data is complicated by the fact that—according to TALYS—the (α, p_0) channel is relatively weak in the $^{17}\text{F}(\alpha, p)^{20}\text{Ne}$ reaction. The predicted branching

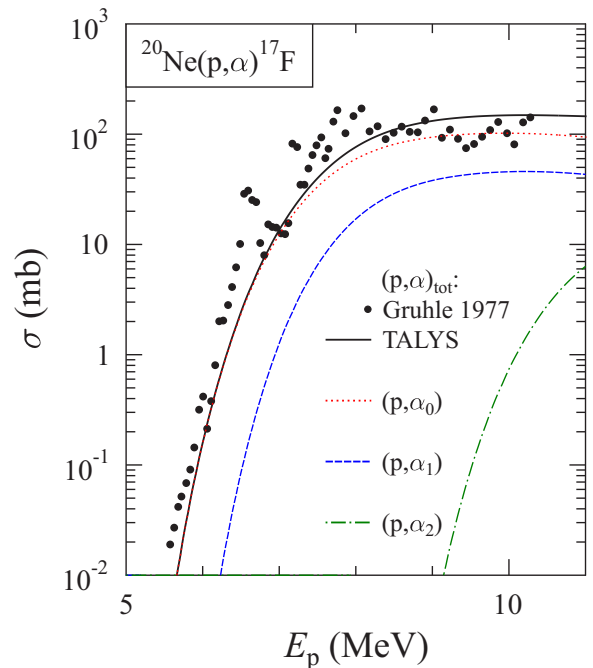


FIG. 6. Experimental cross section of the $^{20}\text{Ne}(p, \alpha)^{17}\text{F}$ reaction [30] in comparison with a statistical model calculation. Similar to the $^{20}\text{Ne}(n, \alpha)^{17}\text{O}$ reaction, because of the dominating α_0 channel the (p, α) data provide an additional constraint for the $^{17}\text{F}(\alpha, p_0)^{20}\text{Ne}$ cross section.

ratios and consequences for the analysis of the experimental data will be presented in Ref. [16]. Note that high-lying excited states in ^{20}Ne from the $^{17}\text{F}(\alpha, p)^{20}\text{Ne}$ reaction may decay to $^{16}\text{O} + \alpha$ before the residual ^{20}Ne nucleus can be detected in the MUSIC chamber at ANL; this complication remained negligible in the analysis of the $^{17}\text{O}(\alpha, n)^{20}\text{Ne}$ data [24] because of the small Q value of the (α, n) reaction.

V. ASTROPHYSICAL REACTION RATES

The astrophysical reaction rate $N_A \langle \sigma v \rangle$ is essentially an average cross section where the averaging is weighted by the thermal Maxwell–Boltzmann distribution of the colliding nuclei. For a given temperature T (typically given as $T_9 = T/10^9$ K) the reaction rate $N_A \langle \sigma v \rangle$ is dominated by the cross section in the so-called Gamow window which is located around $E_0 = 1150$ keV (1820 keV; 2390 keV) for $T_9 = 1$ ($T_9 = 2; 3$) for ^{17}O and ^{18}O and has a width Δ of about 725 keV (1295 keV; 1815 keV) in the center-of-mass system [39,40]. Note that the simple Gamow-window approach does not hold for the $^{18}\text{O}(\alpha, n)^{21}\text{Ne}$ reaction at very low temperatures because of the negative Q value of about -0.7 MeV.

Obviously, the statistical model calculations should be able to provide the reaction rate $N_A \langle \sigma v \rangle$ at high temperatures where the cross section in the Gamow window is composed of a sufficiently high number of resonances. This definitely holds for energies above about 3–4 MeV where the averaged cross sections, such as, e.g., measured by Hansen *et al.* [19] or Avila *et al.* [24], show a smooth energy dependence (see Figs. 1 and 2). Thus, the statistical model is definitely valid at the

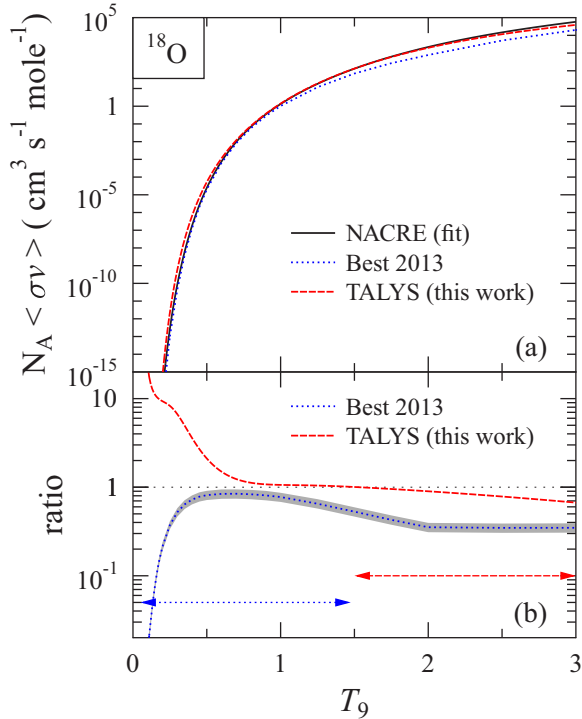


FIG. 7. Reaction rate $N_A\langle\sigma v\rangle$ of the $^{18}\text{O}(\alpha, n)^{21}\text{Ne}$ reaction from the NACRE compilation, from the experimental resonance properties by Best *et al.* [29], and from the statistical model calculations using TALYS. The upper part (a) shows the rates $N_A\langle\sigma v\rangle$; the lower part (b) shows the rates normalized to the NACRE fit, including horizontal arrows which indicate the approximate validity of the different rates. For further discussion see text.

corresponding temperatures slightly above $T_9 = 3$. At lower temperatures down to about $T_9 = 1$ still several resonances are located in the Gamow window. Here $N_A\langle\sigma v\rangle$ from the statistical model should remain more or less reliable (say within a factor of two or so) because $N_A\langle\sigma v\rangle$ approximately averages over the relatively broad Gamow window. This reliability of $N_A\langle\sigma v\rangle$ from the statistical model is confirmed by the reasonable agreement with the experimental rates which are calculated from the sum over the contributing resonances for the nuclei under study. However, below $T_9 \approx 1$, $N_A\langle\sigma v\rangle$ is dominated by very few individual resonances. Here the statistical model is not able to predict $N_A\langle\sigma v\rangle$ with sufficient accuracy.

The reaction rate $N_A\langle\sigma v\rangle$ increases dramatically with temperature. For better visibility, in the following Figs. 7 and 8 the reaction rates $N_A\langle\sigma v\rangle$ are normalized to a reference rate which is taken from the $N_A\langle\sigma v\rangle$ fit functions of the NACRE compilation for ^{17}O and ^{18}O . The rates will be discussed with a focus on the low-temperature region which corresponds to the astrophysical *s* process.

A. $^{18}\text{O}(\alpha, n)^{21}\text{Ne}$

The latest calculation of $N_A\langle\sigma v\rangle$ for the reaction $^{18}\text{O}(\alpha, n)^{21}\text{Ne}$ by Best *et al.* [29] is based on an *R*-matrix analysis of the experimental data, which cover an energy range

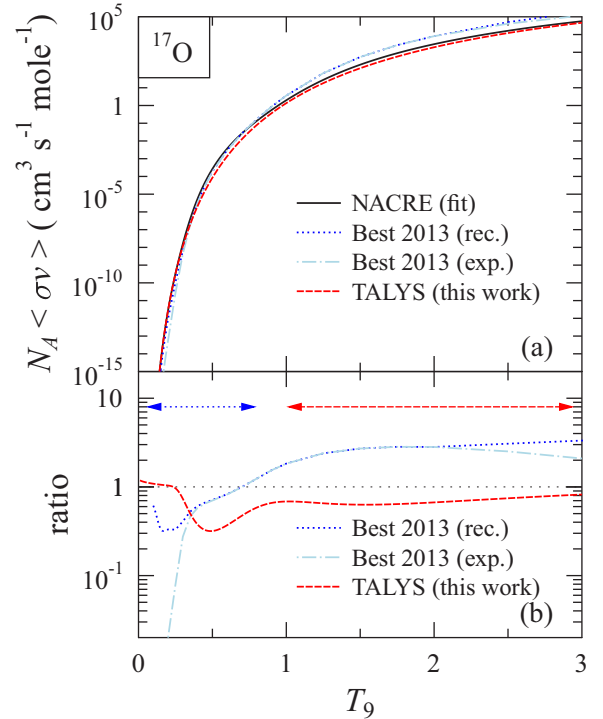


FIG. 8. Reaction rate $N_A\langle\sigma v\rangle$ of the $^{17}\text{O}(\alpha, n)^{20}\text{Ne}$ reaction from the NACRE compilation, from the experimental resonance properties by Best *et al.* [23], and from the statistical model calculations using TALYS. The upper part (a) shows the rates $N_A\langle\sigma v\rangle$; the lower part (b) shows the rates normalized to the NACRE fit, including horizontal arrows which indicate the approximate validity of the different rates. For further discussion see text.

from the threshold up to about 2 MeV; i.e., the Gamow window is fully covered (including the width Δ) up to $T_9 \approx 1.5$. Therefore, at higher temperatures the rate $N_A\langle\sigma v\rangle$ is calculated from the statistical model which has been scaled to $N_A\langle\sigma v\rangle$ from experiment at $T_9 = 2$. The Best results are slightly lower than NACRE, but the deviation does not exceed a factor of two for $0.5 \lesssim T_9 \lesssim 2.0$. The significantly lower $N_A\langle\sigma v\rangle$ at very low temperatures below $T_9 = 0.5$ results from the fact that the lowest resonance in the Denker data at 888 keV is considered as spurious and has been assigned to the $^{17}\text{O}(\alpha, n)^{20}\text{Ne}$ reaction by Best *et al.* [23]. The results are shown in Fig. 7.

The TALYS calculation is between the NACRE rate and the Best rate for temperatures above $T_9 \approx 1$, and it remains closer to the NACRE rate. As pointed out above, at temperatures above $T_9 \approx 3$ the statistical model should be fully valid. Two potential explanations (or a combination of both) can be given for the deviation between the Best rate and the TALYS rate: (i) The number of resonances in the $^{18}\text{O}(\alpha, n)^{21}\text{Ne}$ reaction may be accidentally low in the Gamow window for $T_9 = 2$ around 2 MeV, leading to a scaling factor significantly below 1.0 in Ref. [29] for the adjustment of the statistical model calculations. (Unfortunately, this factor is not provided in Ref. [29]). (ii) The Gamow window at $T_9 = 2$ is not fully covered by the experimental cross sections, leading to a slight

underestimation of $N_A\langle\sigma v\rangle$ at $T_9 = 2$ because of missing contributions from energies above 2 MeV.

At very low temperatures below $T_9 \approx 0.7$ the limitations of the statistical model become clearly visible. The statistical model gives an almost constant astrophysical S factor of $S(E) \approx 3 \times 10^7$ MeV b down to the threshold of the (α, n) reaction. Such a constant S factor leads to a significantly enhanced reaction rate $N_A\langle\sigma v\rangle$ which is excluded by the experimental data of Denker and Best. Note that the negative Q value and the resulting threshold for the (α, n) reaction lead to a relatively well-constrained reaction rate $N_A\langle\sigma v\rangle$ because resonances at very low energies with their typically tiny (and often not measurable) resonance strengths cannot exist.

Summarizing the above, the reaction rate $N_A\langle\sigma v\rangle$ of the $^{18}\text{O}(\alpha, n)^{21}\text{Ne}$ reaction is well-defined down to low temperatures from the Best data. Except for the spurious resonance at 888 keV, the Denker data and also the Bair and the Hansen data at higher energies show good agreement and thus confirm the recommended rate by Best *et al.* [29]. The TALYS calculation cannot be used below $T_9 \approx 0.7$. Above $T_9 \approx 2$ the TALYS calculation gives slightly higher $N_A\langle\sigma v\rangle$. Here the TALYS calculation reproduces the experimental (α, n) data of Bair62, Bair, and Hansen, and is close to the evaluation in the NACRE compilation; thus, the TALYS calculation should be reliable.

B. $^{17}\text{O}(\alpha, n)^{20}\text{Ne}$

Similar to the $^{18}\text{O}(\alpha, n)^{21}\text{Ne}$ reaction, Best *et al.* [23] provide the reaction rate $N_A\langle\sigma v\rangle$ of the $^{17}\text{O}(\alpha, n)^{20}\text{Ne}$ reaction from an R -matrix fit to their experimental data in the energy range from 0.7 to 1.9 MeV. Two versions of $N_A\langle\sigma v\rangle$ are listed in Ref. [23]. The so-called experimental rate $N_A\langle\sigma v\rangle_{\text{exp}}$ is calculated from the experimental resonance strengths (excluding contributions from resonances outside the experimental energy range from 0.7 to 1.9 MeV). The recommended rate $N_A\langle\sigma v\rangle_{\text{rec}}$ additionally includes estimates for low-lying resonances, and at higher temperatures the result of a statistical model calculation is recommended which has been adjusted to the experimental $N_A\langle\sigma v\rangle_{\text{exp}}$ at $T_9 = 2$ [as in the case of the $^{18}\text{O}(\alpha, n)^{21}\text{Ne}$ reaction].

Figure 8 shows the results. As discussed in Sec. III, the Best cross sections are significantly above the other data from the literature; in particular for the (α, n_0) channel above the (α, n_1) threshold. This leads to an enhanced $N_A\langle\sigma v\rangle$ by about a factor of three for $1 \leq T_9 \leq 2$. As expected, above $T_9 = 2$ the enhancement of $N_A\langle\sigma v\rangle_{\text{exp}}$ decreases because of missing contributions from outside the experimental energy range, whereas $N_A\langle\sigma v\rangle_{\text{rec}}$ remains a factor of three above the NACRE rate. The TALYS calculation agrees almost perfectly with the NACRE compilation, and the temperature dependence is almost identical to $N_A\langle\sigma v\rangle_{\text{rec}}$ of Best *et al.* [23], at least for temperatures above $T_9 = 1$.

At very low temperatures, $N_A\langle\sigma v\rangle$ is governed by few low-lying resonances which have not been seen in (α, n) experiments to date. NACRE extends the lowest experimental S -factor data by using a constant $S(E)$ down to $E = 0$. Consequently, the experimental $N_A\langle\sigma v\rangle_{\text{exp}}$ by Best *et al.* is by far below the NACRE result and the TALYS calculation. The recommended $N_A\langle\sigma v\rangle_{\text{rec}}$ is closer to the NACRE rate, but still

about a factor of two lower. The agreement between the TALYS calculation and NACRE for the lowest temperatures is not surprising because the calculated TALYS S factor toward $E \approx 0$ is close to the chosen constant S factor of NACRE. The rough agreement between the Best recommendation and the TALYS rate at low temperatures must be considered as somewhat accidental. However, as the Best-recommended $N_A\langle\sigma v\rangle_{\text{rec}}$ is based on well-chosen average properties of several unobserved low-lying resonances, the resulting $N_A\langle\sigma v\rangle_{\text{rec}}$ should not deviate by orders of magnitude from a statistical model calculation which is also based on average properties. For completeness it can be noted that a microscopic calculation of the $^{17}\text{O}(\alpha, n)^{20}\text{Ne}$ cross section at low energies [41] gives a rate $N_A\langle\sigma v\rangle$ which is more than one order of magnitude lower than the NACRE recommendation at $T_9 \approx 0.1$ [22].

In summary, the reaction rate $N_A\langle\sigma v\rangle$ of the $^{17}\text{O}(\alpha, n)^{20}\text{Ne}$ reaction has significant uncertainties. At low temperatures ($T_9 \lesssim 0.7$) the recommended rate $N_A\langle\sigma v\rangle_{\text{rec}}$ of Best *et al.* is a good choice. Here improved experimental resonance strengths for the yet unobserved low-lying resonances could reduce the uncertainties. However, above $T_9 = 1$ the contradictory experimental data lead to uncertainties of at least a factor of three. Here the Best-recommended $N_A\langle\sigma v\rangle_{\text{rec}}$ should be considered as an upper limit for $N_A\langle\sigma v\rangle$, and the lower limit for $N_A\langle\sigma v\rangle$ should be taken from the NACRE compilation or from the present TALYS calculation. A reduction of this uncertainty requires the resolution of the contradictory experiments.

VI. SENSITIVITY TO THE CHOSEN α -NUCLEUS POTENTIAL

It has been shown that the calculation of cross sections of (α, n) cross sections in the $20 \leq A \leq 50$ mass range is mainly sensitive to the chosen α -nucleus potential [9]. This also holds for the present study for ^{17}O and ^{18}O where the (α, p) channel remains closed up to more than 5 MeV, thus minimizing the role of the nucleon-nucleus potential. Whereas in the $20 \leq A \leq 50$ mass range the McFadden–Satchler potential [10] provides good results [9] and a relative small sensitivity of the reaction cross sections on the α -nucleus potential was seen recently for ^{64}Zn [42], for heavy targets typically huge deviations are found from calculations of different α -nucleus potentials (see, e.g., Refs. [43–45]).

Excitation functions for the $^{18}\text{O}(\alpha, n)^{21}\text{Ne}$ and $^{17}\text{O}(\alpha, n)^{20}\text{Ne}$ reactions were calculated from several α -nucleus potentials. For presentation, the calculated excitation functions are normalized to the reference calculation by using the McFadden–Satchler potential [10] (see Fig. 9).

The following potentials were investigated: The TALYS default potential is based on Watanabe [46] and results in slightly higher cross sections. Similar findings are obtained from Avrigeanu *et al.* [13] which will be used as default in the next TALYS versions. Three different versions, provided by Demetriou *et al.* [11], are also shown in Fig. 9. Whereas the first two versions give cross sections slightly above McFadden–Satchler, the third version is slightly lower; in particular for ^{18}O at low energies.

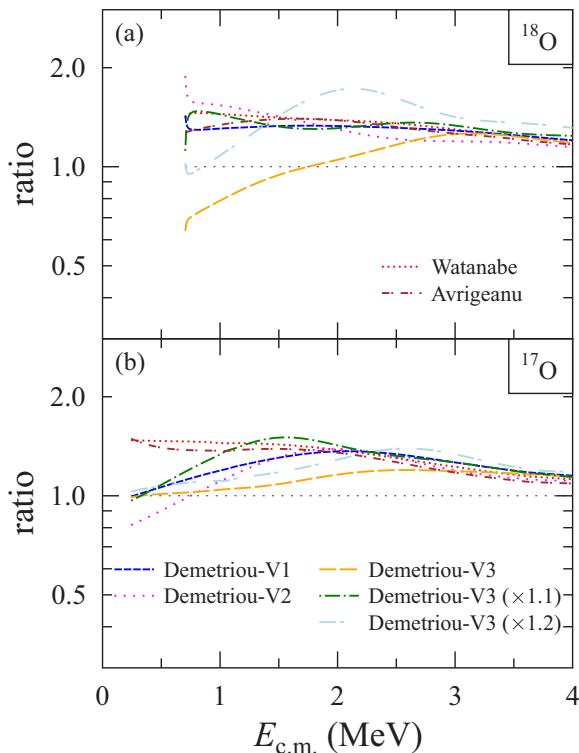


FIG. 9. Ratio between the calculated (α, n) cross sections, normalized to the standard potential of McFadden and Satchler [10], using different α -nucleus potentials for (a) ^{18}O and (b) ^{17}O . The calculated cross sections do not vary by more than a factor of two.

Recently, it has been suggested to multiply the real potential of the third version of Demetriou *et al.* by a factor of 1.1–1.2 [47]. Later, the same factor has been applied in Ref. [15], and good agreement for several reactions was found (see supplement of Ref. [15]). The corresponding calculations using the Demetriou-V3 potential multiplied by 1.1 or 1.2 are also slightly higher than the McFadden–Satchler result.

For completeness, it has to be noted that most of the global potentials [11–13, 15] have been optimized for medium-mass and heavy targets which may lead to additional uncertainties for the light targets under study in this work. For the ATOMKI-V1 potential [12] it is explicitly stated that it is applicable only above $A \gtrsim 60$; thus, the results from ATOMKI-V1 are not included in Fig. 9.

Usually, at higher energies different α -nucleus potentials show a trend to provide almost identical reaction cross sections with small deviations of the order of 10%–20%. Such a

convergence is already found at about 4 MeV for $^{18}\text{O}(\alpha, n)^{21}\text{Ne}$ and $^{17}\text{O}(\alpha, n)^{20}\text{Ne}$ (see Fig. 9). But interestingly also at lower energies the differences from the various α -nucleus potentials remain quite limited within about a factor of two.

VII. CONCLUSIONS

The present study shows that statistical model calculations in combination with the simple α -nucleus potential by McFadden–Satchler are able to reproduce the cross sections of α -induced reactions even for light nuclei with masses $A \lesssim 20$. Obviously, this result holds mainly for higher energies above a few MeV. At lower energies the statistical model cannot reproduce the individual resonances but is still able to reproduce the average trend of the energy dependence which is essential for the prediction of astrophysical reaction rates $N_A \langle \sigma v \rangle$. These results extend the conclusions of Ref. [9] towards lighter nuclei. The results from other recent α -nucleus potentials do not differ by more than a factor of two from the widely used McFadden–Satchler potential.

The statistical model calculations can be used to predict astrophysical reaction rates $N_A \langle \sigma v \rangle$ for higher temperatures above $T_9 \approx 2$ –3 with high reliability. However, as expected, at very low temperatures below $T_9 \approx 1$ the statistical model predictions are not reliable because the reaction rates are governed here by the properties of very few individual resonances.

For the $^{18}\text{O}(\alpha, n)^{21}\text{Ne}$ reaction good agreement between all experimental data is found, leading to an experimentally well-constrained reaction rate $N_A \langle \sigma v \rangle$. Surprisingly, for the $^{17}\text{O}(\alpha, n)^{20}\text{Ne}$ reaction a significant discrepancy has been found at energies above the (α, n_1) threshold between the data by Best *et al.* [23] and several other (α, n) [19–22, 24] and (n, α) [25–28] data sets. This experimental discrepancy has to be resolved for a better definition of the $^{17}\text{O}(\alpha, n)^{20}\text{Ne}$ rate at higher temperatures above $T_9 \approx 1$. For the astrophysically most important low temperatures below $T_9 = 1$ which are typical for the *s* process, the recommendations of Best *et al.* [23] remain valid.

ACKNOWLEDGMENTS

I thank M. Avila and K. E. Rehm for motivating this study and for providing their preliminary data for ^{17}F . Encouraging discussions with A. Best, R. deBoer, and M. Wiescher are gratefully acknowledged. This work was supported by OTKA (Grants No. K108459 and No. K120666).

[1] F. Käppeler, R. Gallino, S. Bisterzo, and W. Aoki, *Rev. Mod. Phys.* **83**, 157 (2011).
 [2] I. Baraffe, M. El Eid, and N. Prantzos, *Astron. Astroph.* **258**, 357 (1992).
 [3] P. Mohr, C. Heinz, M. Pignatari, I. Dillmann, A. Mengoni, and F. Käppeler, *Astroph. J.* **827**, 29 (2016).
 [4] J. Pereira and F. Montes, *Phys. Rev. C* **93**, 034611 (2016).
 [5] P. Mohr, *Phys. Rev. C* **94**, 035801 (2016).

[6] J. Bliss, A. Arcones, F. Montes, and J. Pereira, *J. Phys. G* **44**, 054003 (2017).
 [7] T. Rauscher, N. Nishimura, R. Hirschi, G. Cescutti, A. St. J. Murphy, and A. Heger, *Mon. Not. R. Astron. Soc.* **463**, 4153 (2016).
 [8] A. Simon, M. Beard, B. S. Meyer, and B. Roach, *J. Phys. G* **44**, 064006 (2017).
 [9] P. Mohr, *Eur. Phys. J. A* **51**, 56 (2015).

- [10] L. McFadden and G. R. Satchler, *Nucl. Phys.* **84**, 177 (1966).
- [11] P. Demetriou, C. Grama, and S. Goriely, *Nucl. Phys. A* **707**, 253 (2002).
- [12] P. Mohr, G. G. Kiss, Zs. Fülöp, D. Galaviz, Gy. Gyürky, and E. Somorjai, *At. Data Nucl. Data Tables* **99**, 651 (2013).
- [13] V. Avrigeanu, M. Avrigeanu, and C. Manaiescu, *Phys. Rev. C* **90**, 044612 (2014).
- [14] X.-W. Su and Y.-L. Han, *Int. J. Mod. Phys. E* **24**, 1550092 (2015).
- [15] P. Scholz, F. Heim, J. Mayer, C. Münker, L. Netterdon, F. Wombacher, and A. Zilges, *Phys. Lett. B* **761**, 247 (2016).
- [16] M. L. Avila *et al.* (unpublished).
- [17] M. L. Avila and K. E. Rehm (private communication).
- [18] J. C. Blackmon *et al.*, presentation at NPA-8, Catania, Italy, June 18–23 (2017).
- [19] L. F. Hansen, J. D. Anderson, J. W. McClure, B. A. Pohl, M. L. Stelts, J. J. Wesolowski, and C. Wong, *Nucl. Phys. A* **98**, 25 (1967).
- [20] J. K. Bair and F. X. Haas, *Phys. Rev. C* **7**, 1356 (1973).
- [21] A. B. McDonald, H. B. Mak, H. C. Evans, G. T. Ewan, and H. P. Trautvetter, *Nucl. Phys. A* **273**, 477 (1976).
- [22] A. Denker, Ph.D. thesis, Universität Stuttgart, 1994 (unpublished).
- [23] A. Best, M. Beard, J. Görres, M. Couder, R. deBoer, S. Falahat, R. T. Güray, A. Kontos, K.-L. Kratz, P. J. LeBlanc, Q. Li, S. O'Brien, N. Özkan, M. Pignatari, K. Sonnabend, R. Talwar, W. Tan, E. Uberseder, and M. Wiescher, *Phys. Rev. C* **87**, 045805 (2013).
- [24] M. L. Avila, K. E. Rehm, S. Almaraz-Calderon, A. D. Ayangeakaa, C. Dickerson, C. R. Hoffman, C. L. Jiang, B. P. Kay, J. Lai, O. Nussair, R. C. Pardo, D. Santiago-Gonzalez, R. Talwar, and C. Ugalde, *Nucl. Instrum. Methods Phys. Res., Sect. A* **859**, 63 (2017).
- [25] C. H. Johnson, C. K. Bockelman, and H. H. Barschall, *Phys. Rev.* **82**, 117 (1951).
- [26] R. J. Bell, T. W. Bonner, and F. Gabbard, *Nucl. Phys.* **14**, 270 (1959).
- [27] V. A. Khryachkov, I. P. Bondarenko, B. D. Kuzminov, N. N. Semenova, and A. I. Sergachev, *Phys. At. Nucl.* **75**, 404 (2012).
- [28] V. A. Khryachkov, I. P. Bondarenko, B. D. Kuzminov, N. N. Semenova, A. I. Sergachev, T. A. Ivanova, and G. Giorganis, *EPJ Web Conf.* **21**, 03005 (2012).
- [29] A. Best, S. Falahat, J. Görres, M. Couder, R. deBoer, R. T. Güray, A. Kontos, K.-L. Kratz, P. J. LeBlanc, Q. Li, S. O'Brien, N. Özkan, K. Sonnabend, R. Talwar, E. Uberseder, and M. Wiescher, *Phys. Rev. C* **87**, 045806 (2013).
- [30] W. Gruhle and B. Kober, *Nucl. Phys. A* **286**, 523 (1977).
- [31] EXFOR data base, available online at <http://www-nds.iaea.org/exfor>.
- [32] A. J. Koning, S. Hilaire, and S. Goriely, computer code TALYS, <http://www.talys.eu>.
- [33] P. Mohr, Gy. Gyürky, and Zs. Fülöp, *Phys. Rev. C* **95**, 015807 (2017).
- [34] C. Angulo *et al.*, *Nucl. Phys. A* **656**, 3 (1999).
- [35] Y. Xu, K. Takahashi, S. Goriely, M. Arnould, M. Ohta, and H. Utsunomiya, *Nucl. Phys. A* **918**, 61 (2013).
- [36] J. K. Bair and H. B. Willard, *Phys. Rev.* **128**, 299 (1962).
- [37] A. Best, R. deBoer, and M. Wiescher (private communication); R. deBoer *et al.*, presentation at NPA-8, Catania, Italy, June 18–23 (2017).
- [38] F. D. Becchetti, R. S. Raymond, R. O. Torres-Isea, A. Di Fulvio, S. D. Clarke, S. A. Pozzi, and M. Febraro, *Nucl. Instrum. Methods Phys. Res., Sect. A* **820**, 112 (2016).
- [39] C. E. Rolfs and W. S. Rodney, *Cauldrons in the Cosmos* (The University of Chicago Press, Chicago, 1988).
- [40] C. Iliadis, *Nuclear Physics of Stars* (Wiley-VCH, Weinheim, 2007).
- [41] P. Descouvemont, *Phys. Rev. C* **48**, 2746 (1993).
- [42] A. Ornelas, P. Mohr, Gy. Gyürky, Z. Elekes, Zs. Fülöp, Z. Halász, G. G. Kiss, E. Somorjai, T. Szücs, M. P. Takács, D. Galaviz, R. T. Güray, Z. Korkulu, N. Özkan, and C. Yalçın, *Phys. Rev. C* **94**, 055807 (2016).
- [43] E. Somorjai, Zs. Fülöp, A. Z. Kiss, C. E. Rolfs, H.-P. Trautvetter, U. Greife, M. Junker, S. Goriely, M. Arnould, M. Rayet, T. Rauscher, and H. Oberhummer, *Astron. Astrophys.* **333**, 1112 (1998).
- [44] D. Galaviz, Zs. Fülöp, Gy. Gyürky, Z. Máté, P. Mohr, T. Rauscher, E. Somorjai, and A. Zilges, *Phys. Rev. C* **71**, 065802 (2005).
- [45] A. Sauerwein, H. W. Becker, H. Dombrowski, M. Elvers, J. Endres, U. Giesen, J. Hasper, A. Hennig, L. Netterdon, T. Rauscher, D. Rogalla, K. O. Zell, and A. Zilges, *Phys. Rev. C* **84**, 045808 (2011).
- [46] S. Watanabe, *Nucl. Phys.* **8**, 484 (1958).
- [47] L. Netterdon, J. Mayer, P. Scholz, and A. Zilges, *Phys. Rev. C* **91**, 035801 (2015).